Are sudden stratospheric warmings preceded by anomalous tropospheric wave activity?

Alvaro de la Cámara*

Dept. Earth Physics and Astrophysics, Universidad Complutense de Madrid, Spain

Institute of Geosciences, CSIC-UCM, Madrid, Spain

Thomas Birner

Meteorological Institute Munich, University of Munich, Germany

John R. Albers

Cooperative Institute for Research in Environmental Sciences(CIRES), University of Colorado, Boulder, Colorado, USA

Physical Sciences Division, NOAA/Earth System Research Laboratory, Boulder, Colorado, USA

**Corresponding author address:* Dept. Earth Physics and Astrophysics, Universidad Complutense de Madrid, Plaza de las Ciencias 1 28040, Madrid, Spain.

E-mail: acamarai@ucm.es

ABSTRACT

A combination of 20th century reanalysis products and 240 years of output from a state-of-the-art chemistry climate model are used to investigate to what extent sudden stratospheric warmings are preceded by *anomalous* tropospheric wave activity. To this end we study the fate of lower tropospheric wave events (LTWEs) and their interaction with the stratospheric mean flow. These LTWEs are contrasted with sudden stratospheric deceleration events (SSDs), which are similar to sudden stratospheric warmings (SSWs) but place more emphasis on the explosive dynamical nature of these events. Reanalysis and model output provide very similar statistics: Around one third of the SSDs identified are preceded by wave events in the lower troposphere, while two thirds of the SSDs are not preceded by a tropospheric wave event. In addition, only 20% of all anomalous tropospheric wave events are followed by an SSD in the stratosphere. This constitutes statistically significant evidence that the anomalous amplification of wave activity in the stratosphere that drives SSDs is not necessarily due to an anomalous amplification of the waves in the source region (i.e. the lower troposphere). The results suggest that the dynamics in the lowermost stratosphere and the vortex geometry are essential, and should be carefully analyzed in the search for precursors of SSDs.

1. Introduction

Sudden stratospheric warmings (SSWs) are major disruptions of the wintertime stratospheric polar vortex of the Northern Hemisphere (Labitzke 1977; Butler et al. 2015), which profoundly alter the stratospheric circulation and transport at global scale (see de la Cámara et al. 2018a,b, and references therein). Perhaps the most important impact of SSWs in terms of potential societal repercussions is their influence on Euro-Atlantic weather regimes: the associated stratospheric temperature and wind anomalies during SSWs can induce changes in the storm track that impact surface weather for up to two months (Baldwin and Dunkerton 2001; Thompson et al. 2002; Kidston et al. 2015; Ayarzagüena et al. 2018). Indeed, increasing evidence suggests that SSWs are a source of additional predictability in subseasonal-to-seasonal forecasting of winter climate in Europe and eastern North America (Marshall and Scaife 2010; Smith and Kushner 2012; Tripathi et al. 2015; Scaife et al. 2016).

In this context, understanding the still unclear mechanisms behind the explosive growth of stratospheric wave activity that ultimately triggers SSWs arises as a major scientific question. In particular, much of the discussion centers on the relative roles of tropospheric and stratospheric processes in the wave flux amplification that happens in the stratosphere. On one hand, the planetary Rossby waves present in the stratosphere have their primary sources in the troposphere (Andrews et al. 1987). Therefore, an often-invoked explanation for the rapid increase of stratospheric wave fluxes is the anomalous excitation of these waves in the troposphere and their subsequent propagation into the stratosphere (e.g., Matsuno 1971; Polvani and Waugh 2004). In this context, several phenomena have been linked with an increased probability of SSW occurrence, such as El Niño-Southern Oscillation (ENSO), the Quasi-Biennial Oscillation (QBO), the Madden-Julian Oscillation (MJO), blockings, etc. (e.g., Butler and Polvani 2011; Scaife et al. 2014; Domeisen

et al. 2018a; Garfinkel et al. 2012, 2018; Martius et al. 2009; Barriopedro and Calvo 2014; Colucci and Kelleher 2015). On the other hand, stratospheric conditions may crucially determine the occurrence of an SSW by modulating the propagation of wave activity from the troposphere, developing its own internal instabilities, or even favoring resonant wave amplification (e.g., Clark 1974; Plumb 1981; McIntyre 1982; Chen and Robinson 1992; Christiansen 1999). Experiments with highly truncated stratosphere-only models (i.e., with inactive troposphere) have suggested that the stratosphere is able to internally generate oscillations that resemble SSWs (e.g., Holton and Mass 1976; Yoden 1987; Scott and Haynes 2000; Chen et al. 2001; Matthewman and Esler 2011; Esler and Matthewman 2011). In particular, Sjoberg and Birner (2014) have demonstrated the ability of such a model stratosphere to internally generate an SSW even with constant prescribed bottom boundary wave activity flux. But to what extent is this applicable to more complex global models, or even to reality, where there is strong transient forcing from the troposphere? Although pointing to different of the above-mentioned mechanisms in their explanation of the stratospheric wave activity amplification, simulations with three-dimensional primitive equation models of the stratosphere (Smith 1989, 1992; Martineau et al. 2018a), global dry dynamical core models (Scott and Polvani 2004; Hitchcock and Haynes 2016; Jucker 2016; Martineau et al. 2018a; Lindgren et al. 2018), and state-of-the-art general circulation models (Christiansen 1999; Scott and Polvani 2006; de la Cámara et al. 2017), all point out the ability of the stratosphere to modulate or control the occurrence of, and even internally generate, SSWs.

There are also studies that use reanalysis products to gain new insights into the relative roles of anomalous tropospheric wave injection and stratospheric control on the explosive growth of stratospheric wave activity that triggers SSWs. In particular, Birner and Albers (2017) (BA17 hereafter) used 38 years of reanalysis fields to reveal that only about 33% of the observed SSWs since 1979 were preceded by anomalously strong lower tropospheric wave events, and that only

20% of the lower tropospheric wave events are followed by SSWs. These results give context to recent case studies that have provided evidence of the essential role of the stratosphere state (i.e. vortex preconditioning) in the development of the SSWs of 2009 (Albers and Birner 2014; Domeisen et al. 2018b) and 2013 (Attard et al. 2016).

The goal of the present paper is to expand the study of BA17, and investigate if SSWs are preceded by anomalous tropospheric wave activity in long climate records. We will use historical climate simulations of the Whole Atmosphere Community Climate Model (WACCM) and data from the European Reanalysis 20th Century (ERA-20C). We identify lower tropospheric events of anomalously strong wave activity, as well as mid-stratospheric events of strong zonal wind deceleration. Our results show that only $\sim$1/5 of tropospheric wave events are followed by stratospheric events, and that about 1/3 of stratospheric events are preceded by tropospheric wave events. Composite analyses of the upward wave activity flux provide evidence that the rapid amplification of stratospheric wave fluxes that drives SSWs can hardly be attributed to amplification in the tropospheric wave sources, at least in a composite sense. Analysis of the vortex moment diagnostics suggests that the vortex is preferentially wider and center over the pole before stratospheric events dominated by zonal wavenumber 1 amplification.

The remainder of the paper is organized as follows. Section 2 describes the model output, methods and diagnostics employed, while section 3 presents the results. A summary and discussion of the main results are included in section 4.

2. Data and Methods

a. Model output and reanalysis

In this study we use output from a state-of-the-art chemistry climate model and a 20th century reanalysis. The model used is the Whole Atmosphere Community Climate Model (WACCM) version 4 (Marsh et al. 2013; Garcia et al. 2017), which can serve as the atmospheric component of the Community Earth System Model developed at the National Center for Atmospheric Research. We use an ensemble of 4 members forced with observed sea surface temperatures and external forcings for the period 1955-2014, with a horizontal resolution of 2.5°x1.9° longitude–latitude, and 66 levels in the vertical with the top at about 140 km altitude. This provides 240 years of daily output.

We also use daily meteorological fields from the European Reanalysis of the 20th century (ERA-20C) (Poli et al. 2016), developed at the European Center for Medium-range Weather Forecast (ECMWF). The horizontal resolution is approximately 125 km and has 91 vertical levels between the surface and 0.01 hPa. In particular we use the zonal-mean data set described in Martineau et al. (2018b). ERA-20C covers the period 1900-2010, assimilating observations of surface pressure and surface winds over the ocean. It is important to remark that ERA-20C is not taken in this study as a reliable reproduction of the synoptic evolution of the stratosphere, but rather as a valuable long dataset from which statistics can be extracted.

In this study the climatological seasonal cycle is computed as a smoothly varying climatology, by calculating 30-year means every 10 years for each month individually and inter- and extrapolating back to a yearly time series (again, for each month individually). Deseasonalized anomalies are then calculated as the difference between the daily fields and the seasonal cycle, after which a 10-day running mean is applied.

b. Identification of events

We have used similar methods to BA17's for the identification of anomalous lower troposphere wave events (LTWE) and SSWs, employing time series of tropospheric wave activity normalized by the interannual standard deviation (referred to as standardized anomalies throughout the paper). For LTWEs, we take the time series of standardized anomalies of F_z at 600 hPa averaged over 45°-75°N. The selection of a different pressure level in the lower troposphere does not affect the results significantly (not shown). Since SSWs tend to be triggered by amplification of individual planetary waves, and previous studies have reported a high degree of anticorrelation between the longest planetary waves (e.g., Labitzke 1978, 1981), this is done separately for the zonal harmonics with wave number 1 ($F_z(s=1)$) and 2 ($F_z(s=2)$). We identify an LTWE when the value of standardized F_z anomalies goes beyond the value corresponding to 2 standard deviations (σ). The central date of the event is taken as the day with the maximum value of F_z, and consecutive events must be at least 20 days apart, which is approximatively two radiative relaxation time scales of the polar mid-stratosphere (Newman and Rosenfield 1997; Charlton and Polvani 2007). With these criteria, there are 191 LTWE1 and 182 LTWE2 in WACCM, and 71 and 91 in ERA-20C, respectively.

For SSWs, we use a metric based on the deceleration of the zonal mean wind at 60°N and 10 hPa, and thus are referred to as sudden stratospheric deceleration (SSD) events. An SSD is identified when the 10-day change in the zonal mean zonal wind falls below -18 $\mathrm{m{\cdot}s^{-1}}$ in WACCM and -20 $\mathrm{m{\cdot}s^{-1}}$ in ERA-20C (which approximately equal 2 standard deviations in each dataset), with the central date set on the day with the strongest deceleration. Again, two consecutive events must be separate by at least 20 days. This procedure is similar to that described in Martineau and Son (2015), and sets the focus on the dynamical event. We identify 200 SSDs in WACCM and 95 in ERA-20C.

We further classify SSDs according to the dominant planetary wave number during the event. Taking the standardized anomalies of F_z at 50 hPa, a wave-1 SSD (SSD1) is classified if $F_z(s=1)$ is larger than 2σ in any day within $\pm$ 5 days from the SSW central date, provided that $F_z(s=2)$ is smaller than 2σ. Conversely, a wave-2 SSD (SSD2) is classified if $F_z(s=2)$ is larger than, and $F_z(s=1)$ is smaller than, 2σ. If both $F_z(s=1)$ and $F_z(s=2)$ meet the 2σ threshold any day within $\pm$ 5 days from the central date, the event is classified as wave-1 and 2 event (SSD1&2). The rest of events, where none $F_z(s=1)$ or $F_z(s=2)$ meet the threshold, are referred to as weak wave SSDs (SSDww).

c. Vortex moment diagnostics

In this study we make use of vortex moments and elliptical diagnostics (Melander et al. 1986; Waugh 1997) to extract time series of the centroid position (λ_c, ϕ_c), area A, and aspect ratio r of the equivalent ellipse. The "equivalent ellipse" is an ellipse of uniform potential vorticity (PV) with the same moment diagnostic as the polar vortex at a given time. For this purpose we use daily mean values of PV at the isentropic surface of 850 K ($\sim$10 hPa) from both WACCM and ERA-20C, and apply the methodology of Matthewman et al. (2009) to compute both the absolute vortex moments M_{kl}

$$M_{kl} = \iint (\hat{q}(x,y) - q_b) x^k y^l dx dy, \tag{1}$$

and the relative vortex moments J_{kl}

$$J_{kl} = \iint (\hat{q}(x,y) - q_b)(x - x_c)^k (y - y_c)^l dx dy. \tag{2}$$

In Eqs. 1 and 2 q is PV, q_b is the vortex boundary taken as the PV average north of 45°N, and $\hat{q}$ is a modified PV field equal to q if $q > q_b$ (i.e. in the vortex interior), and equal to q_b elsewhere.

Note that we have followed Waugh (1997) in the selection of the value of the vortex boundary q_b, and that it was shown in that study that the results were not sensitive to this selection. Also, (x,y) are Cartesian coordinates in the Lambert's azimuthal projection, (k,l) give the moments order in the (x,y) directions, and (x_c,y_c) are the position of the ellipse's centroid defined as:

$$(x_c,y_c) = \frac{1}{M_{00}}(M_{10},M_{01}). \tag{3}$$

With these definitions, the area of the equivalent ellipse is computed as:

$$A = \frac{M_{00}}{q_b}, \tag{4}$$

and the ellipse's aspect ratio as:

$$r = \left| \frac{J_{20}+J_{02}+\sqrt{4J_{11}^2+(J_{20}-J_{02})^2}}{J_{20}+J_{02}-\sqrt{4J_{11}^2+(J_{20}-J_{02})^2}} \right|^{1/2}. \tag{5}$$

The ellipse centroid position (Eq. 3) gives a measure of the displacement of the vortex, the ellipse area (Eq. 4) is an estimation of the vortex's area and strength, and the aspect ratio (Eq. 5) is a measure of the vortex's elongation (i.e. the ratio between the major and minor axes of the vortex). The reader is referred to Matthewman et al. (2009) for further details.

3. The relation between lower tropospheric wave events and sudden stratospheric warmings

a. Are extreme lower tropospheric wave events followed by SSDs?

The first question we address is the fate of anomalously strong lower tropospheric wave events, so we bin the events regarding whether or not they are followed by SSDs in the stratosphere in a time span of 10 days. This time scale of 10 days was found by Sjoberg and Birner (2012) to be associated with the wave forcing of SSWs. Group velocity estimates also motivate this time scale

(see Albers and Birner 2014, and BA17), but note that the results are not very sensitive to making this time scale a bit longer or shorter. Table 1 presents the corresponding statistics. The results are remarkably similar between WACCM and ERA-20C; only 19% of all LTWEs are followed by SSDs in the climate model, and 17% in the reanalysis. Viewed as a function of the individual wavenumber events, 26% of LTWE1 in WACCM and 29% in ERA-20C are followed by SSDs; for LTWE2, 12% and 8% of the events in the respective datasets are followed by SSDs.

Figure 1 shows the evolution of standardized anomalies of F_z (black contours) and zonal wind acceleration (color shading), composited around LTWE1 and LTWE2 followed and not by SSDs in WACCM. By construction, the four composites show a peak in upward wave activity anomalies at 600 hPa at lag 0 days (Figs. 1a-b and 1d-e), with values larger than 2σ. In the stratosphere, there are significant anomalies of wave activity and wind deceleration peaking at positive lags in LTWE1 and LTWE2 events followed by SSDs (Figs. 1a and 1d). Peak values larger than 2σ take place at lag 5 days simultaneously for both variables, but they are centered at 10-20 hPa for wind deceleration and at around 100 hPa for the wave activity. Also, the anomalies of wave activity expand the whole depth of the stratosphere for LTWE1 (Fig. 1a), while they appear more restricted to the lower stratosphere for LTWE2 (Fig. 1d). For the events not followed by SSWs (Figs. 1b and 1e), the anomalies of wave activity in the stratosphere are smaller than 0.5σ, although there is a short period of time at lags 1-4 days with values over 1σ in the lowermost stratosphere (below 100 hPa) for both LTWE1 and LTWE2. These (weaker) anomalies in wave activity do not translate into changes of the stratospheric circulation, the wind acceleration anomalies in the stratosphere remain small (shading in Figs. 1b and 1e). Looking at the composite difference between events followed and not followed by SSDs (Figs. 1c and 1f), it is clear that the main differences are located in the stratosphere, particularly for LTWE1. It is not the case that tropospheric wave events followed by SSDs are stronger, in a composite sense, than those not followed by SSDs.

Figure 2 shows the corresponding composites using ERA-20C. The structure and evolution of the anomalies are quite similar to those in WACCM (Fig. 1), especially for LTWE1 (top row). There are some differences between WACCM and ERA-20 in the composites corresponding to LTWE2 events followed by SSDs (although the number of events in ERA-20C is small) (Figs. 1d and 2d, respectively), such as a deeper extension of the $F_z(s=2)$ anomalies in the stratosphere in the case of ERA-20C. However, the main message extracted from Fig. 1 holds here: Sorting the tropospheric wave events regarding whether or not they are followed by SSDs does not discriminate the amplitude of wave activity anomalies in the troposphere, at least in a composite sense. The main differences, as expected from the construction of the composites, happen in the stratosphere.

BA17 suggested the presence of a wave source above the tropopause in LTWE1 that are followed by SSDs, but they worked with only 7 events of this type in ERA-Interim. Figure 3 displays the evolution of the 10-day running-mean EP flux divergence (EPFD) around LTWEs at $\sim$250 hPa, in both WACCM (top row) and ERA-20C (bottom row). Note that this figure shows the net value of EPFD, not the anomalies. For LTWE1 followed by SSDs (red line in Figs. 3a and 3c), there is a transition from negative EPFD at negative lags (wave dissipation/sink) to positive at positive lags (wave source), consistently with BA17's results. This can be interpreted as a source of wave activity, and may contribute to the rapid growth of stratospheric wave activity in these cases –i.e. LTWE1 followed by SSDs. A possible explanation of a wave source above the tropopause is shear instability (Charney and Stern 1962). A necessary condition for barotropic/baroclinic instability is a reversal of the positive meridional potential vorticity (PV) gradient, but we have not found any signature of this necessary condition in our analysis (not shown). Another possibility for the wave-1 source above the tropopause is wave-wave interactions (Smith 1983; Smith et al. 1984); further research is needed to gain more insights into this wave-1 source.

Next we turn our attention to the evolution of the vortex geometry during LTWEs to better understand why some LTWEs are followed by SSDs while others (the majority) are not. The objective is to explore preconditioning ideas by which the state of the vortex may contribute to the wave activity burst in the stratosphere via modulation/focusing of wave propagation and/or favoring wave resonance (e.g., McIntyre 1982; Smith 1992). Figure 4 shows composite differences between LTWEs followed and not followed by SSDs of the latitude of the vortex centroid (left panels), vortex area (middle panels), and vortex aspect ratio (right panels). In WACCM (upper panels of Fig. 4), the vortex centroid tends to be located 2° to 4° to the north, and to be larger and stronger, during the two weeks prior to LTWE1 when these are followed by SSDs (red lines in Figs. 4a-b). These positional and strength preferences are not found before LTWE2 events (black lines in Fig. 4a-b). At positive lags, the centroid is displaced farther off of the pole and the vortex looses size and strength in wave events followed by SSDs with respect to those not followed by SSWs, as expected. No significant differences are found in the evolution of the vortex's aspect ratio (Fig. 4c). These results suggest that the vortex is preferentially strong and centered on the pole for tropospheric wave-1 events to be followed by SSDs, and therefore puts the spotlight on the stratospheric state to determine whether or not an LTWE will be followed by an SSD.

b. Are SSDs preceded by lower tropospheric wave events?

We next address the problem from the opposite perspective: How many SSD events are preceded by anomalously strong lower tropospheric wave events? (We use here the same 10-day time scale). Table 2 presents the corresponding statistics. As in the previous subsection, the numbers are very similar between WACCM and ERA-20C: 37% of all SSWs are preceded by LTWEs in the climate model, and 33% in the reanalysis. Our results are consistent with ERA-Interim (BA17), as well as with a recent analysis of over 1,500 years of climate model runs where 34% of all simulated SSWs

were preceded by LTWEs (White et al. 2019). Sorting the stratospheric warmings as a function of the dominant wavenumber (see section b), we find that 38% (40%) of SSD1 events are preceded by LTWE1 in WACCM (ERA-20C), while 28% (29%) of SSD2 events are preceded by LTWE2. Note that SSD1 (SSD2) events represent 53% (30%) of all SSDs in WACCM, and 47% (18%) in ERA-20C.

The (standardized) anomalies of $F_z(s{=}1{+}2)$ in the stratosphere present values over 2σ in the ± 5 days of the SSW central date, simultaneously with large wind deceleration anomalies (Figs. 5a,d). This is evidence of the positive feedback internal to the stratosphere (e.g., Sjoberg and Birner 2014) between upward wave activity and the mean flow that leads to SSDs. The composites show much weaker anomalies in the troposphere, slightly over 0.5σ in WACCM and even weaker in ERA-20C (Figs. 5a,d). From this perspective, the amplification of F_z in the stratosphere for the majority of events can hardly be attributed to amplification in the tropospheric wave sources.

Sorting the SSDs regarding the dominant wavenumber reveals that SSD1 events have a stronger tropospheric signal of wave activity than SSD2 events, both in WACCM and ERA-20C (middle and right panels of Fig. 5), with peak anomalies reaching 1σ in the 10 days prior to the stratospheric event (Figs. 5b,e). Given the relatively large sample of SSDs we are working with in both datasets, we can analyze in detail the evolution of the upward wave activity according to whether or not they were preceded by LTWEs. Focusing on SSD1 events first, we see in Fig. 6 that the evolutions of both the upward wave activity in the stratosphere and the deceleration anomalies are very similar in both type of events (i.e. preceded or not by LTWEs). The differences take place in the troposphere, where there is a much stronger wave activity signal if the SSDs are preceded by LTWEs (Figs. 6a,c). Therefore, the composite signal of wave fluxes in the troposphere preceding SSDs (particularly SSD1 events) evident in Figs. 5b,e comes for the most part from a smaller subset of events (38%) with substantial tropospheric wave fluxes (LTWEs), while the remainder

of SSD1 events have quite small lower tropospheric fluxes. However, even in the events not linked to tropospheric wave events there are anomalies over one standard deviation in the upper troposphere, which could be related to recent findings on the relation between tropospheric synoptic events and lower stratospheric heat flux anomalies (Attard and Lang 2019). This happens both in WACCM and ERA-20C. Figure 7 displays the corresponding panels for SSD2 events. The wave activity anomalies in the upper troposphere in cases not preceded by LTWEs are much weaker for SSD2 than SSD1 events, perhaps suggesting that the connection with tropospheric dynamics is weaker for split than for displacement SSDs. Also, the enhancement of wave activity is vertically confined below 10 hPa, but a similar message is conveyed here: The main difference between events preceded and not preceded by LTWEs happens in the troposphere.

The wave-1 source signal that appeared above the tropopause after LTWE1 events followed by SSDs (Figs. 3a,c) shows up as well when compositing as a function of SSD1 events (Fig. 8). The important aspect that Fig. 8 introduces is that this wave-1 source signal is linked to the occurrence of SSD1 events regardless of whether or not they are preceded by LTWEs. This would suggest that processes internal to the stratosphere are playing an important role here.

We next analyze the vortex moment diagnostics in the mid-stratosphere (850 K). Figure 9 shows the composite evolution of the anomalies of the latitude of the centroid, area, and aspect ratio for SSD1 and SSD2 events. For the vortex centroid and area (left and middle panels), there is a clear cycle going from negative to positive lags where the vortex moves away from the pole and shrinks. This is what is expected during the life cycle of sudden warmings. Looking into what happens at negative lags in more detail, we find some differences in the statistical significance of the signals between WACCM and ERA-20C. In the climate model the vortex centroid is significantly located 2° to the north before SSD1 events (Fig. 9a), but in the reanalysis this is not the case (Fig. 9d). On the other hand, the reanalysis shows a significantly stronger and wider vortex up until $\sim$15

days before both SSD1 and SSD2 events (Fig. 9e), as well as an elongated vortex before SSD2 events (Fig. 9f); but these signals are absent in the model. Generally, Fig. 9 shows a wider vortex that tends to be located further to the pole before SSD1 events. To the extent to which SSD1 events will be dominated by displacement sudden warmings (Charlton and Polvani 2007), these results are fairly consistent with previous studies (e.g., Albers and Birner 2014). And importantly, isolating the SSD events that are preceded and not preceded LTWEs does not change statistically significantly our results (see Fig. S1 supplementary material). However, there is a lack of consistency between WACCM and ERA-20C for these vortex moment diagnostics that suggests that preconditioning signals are not very robust.

4. Discussion and Conclusions

We have used 240 years from historical runs with the chemistry-climate model WACCM, and the 20th-century reanalysis ERA-20C to analyze the relation between anomalous lower tropospheric wave events (LTWEs) and the occurrence of sudden stratospheric deceleration (SSD) events, from which sudden stratospheric warmings defined as wind reversals at 60°N and 10 hPa are a subset. Our results robustly show that:

- only $\sim$20% of all LTWEs are followed by an SSD, and

- only $\sim$1/3 of all SSDs are preceded by an LTWE.

These results are not very sensitive to the specific thresholds used in the definitions of both LTWEs and SSDs (not shown).

One might argue that a threshold of (or around) 2σ for the definition of LTWEs is too restrictive, and that SSDs may be more directly linked to anomalous situations in the troposphere of moderate intensity. To check this point, we have selected *moderate* LTWEs (mLTWEs) in WACCM, defined

as those events where the anomalies of upward EP flux are larger than 1σ but stay lower than 2σ. The percentages of mLTWEs followed by SSDs, and of SSDs preceded by mLTWEs, are remarkably similar to our results with extreme LTWEs (see Tables S1 and S2 in the supplementary material). This indicates that the probability of occurrence of SSDs does not depend on the strength of the tropospheric wave activity anomalies, and further highlights the weak statistical connection between SSDs and anomalous wave events in the troposphere.

The consistency found between the model and the 20th-century reanalysis confirms previous results with the shorter record of ERA-Interim (Birner and Albers 2017), and provides statistically significant evidence that the anomalous amplification of wave activity in the stratosphere that drives SSDs is in most cases not due to an anomalous amplification of the waves in the source region (i.e. the lower troposphere). This is consistent with idealized model experiments (e.g., Scott and Polvani 2004, 2006; Christiansen 1999; Matthewman and Esler 2011; Esler and Matthewman 2011; Jucker 2016; Lindgren et al. 2018; de la Cámara et al. 2017; Sjoberg and Birner 2014), and demonstrated here in reanalysis and state-of-the-art chemistry climate model simulations (see also White et al. 2019). If anomalous tropospheric wave activity does not represent the main cause of the sudden rise of stratospheric upward EP fluxes, which process does? The answers that previous research offers give a primary role to the stratospheric circulation. Birner and Albers (2017) argued that the climatological wave activity in the troposphere is around one order of magnitude larger than in the stratosphere, so it may well be enough to tap into this reservoir below for the stratosphere to develop an SSW (see SSD composites of the net wave fluxes –no anomalies– in Figs. S2 and S3 of Supplementary material). This can be achieved with lower stratospheric configurations that allow extra penetration of the tropospheric wave activity (Chen and Robinson 1992), but also with a vortex geometry that favors the focusing of wave activity towards high latitudes (McIntyre 1982). Although it has been proven hard to diagnose (Albers and Birner 2014;

Domeisen et al. 2018b), resonance is another process explaining rapid wave amplification in the stratosphere linked to SSWs (Clark 1974; Tung and Lindzen 1979; Plumb 1981; Matthewman and Esler 2011).

Within this context, we have employed vortex moment diagnostics and shown that the vortex is generally wider and located closer to the pole before wave-1 LTWEs (LTWE1) that are followed by SSDs (Fig.4); a configuration found to precede wave-1 SSDs (SSD1) in a composite sense, regardless of whether they are or not connected to LTWEs (Fig. 9). We have also found that LTWE1 followed by SSD1 events are generally accompanied by a wave-1 source just above the tropopause (Fig. 3), something found as well for the composite of all SSD1 events (Fig. 8). The reason for this wave source region is unclear, and conditions for shear instability are hardly met in our composite analysis (not shown), which calls for further research.

Our results in Figs. 5, 6 and 7 suggest the majority of stratospheric events do not trace back to anomalously strong tropospheric wave forcing. One would then expect ERA-20C, which only includes assimilation of surface observations, to do poorly in simulating the correct timing of stratospheric events such as SSDs. We have compared event dates in ERA-20C to those found in ERA-Interim by BA17 (see Table S3 in supplemental material) for the common period of 1979-2010. Surprisingly, 10 out of 27 SSDs found in ERA-Interim are reproduced to within 3 days by ERA-20C. Furthermore, for many of the remaining 17 SSD events the evolution of the zonal mean zonal wind at 60° and 10 hPa is remarkably similar between ERA-20C and ERA-Interim (not shown). Nevertheless, there are striking counter-examples where the event is essentially missed completely in ERA-20C, such as the January 2009 SSW, which was previously interpreted to have been triggered by resonance (Albers and Birner 2014).

Is the knowledge of the near-surface wave fluxes and their correct evolution (likely to be the case in ERA-20C) sufficient then to reproduce SSDs in many cases? First, note that 5 out of the

subset of 10 common SSD events between the data sets are associated with an LTWE (see Table 1 in supplemental material of BA17), which may indicate that these 5 events were indeed triggered by a pulse of anomalously strong upward wave flux from the lower troposphere. However, we also note that the stratospheric state prior to SSDs is essentially a function of the history of wave fluxes of tropospheric origin and their (non-trivial) interactions with the stratospheric mean flow. More or less constraining the *evolution* of lower tropospheric wave fluxes in ERA-20C will likely 'nudge' the entire column toward the observed state. Furthermore, it is important to note that data assimilation (such as the 4DVar system used for ERA-20C) can be quite powerful in adjusting the flow field remote to the region of data input. For example, Compo et al. (2006) showed how assimilating a single surface measurement that is only 1 hPa different from the model 'first guess' produces a vertically deep response all the way up to at least 300 hPa. The implication is that data assimilation of surface observations, particularly those of surface pressure, has a far field effect that likely effectively constrains the wave flux evolution of the entire troposphere. Nevertheless, the fact that more than half of the observed SSDs between 1979-2010 are not captured in ERA-20C means that the non-linearity of the positive wave-mean flow feedback leading to SSDs (and SSWs) may break the above mentioned effective constraints and thereby limit the predictability of SSDs.

The search for precursors of sudden stratospheric warmings is in good part motivated by the additional skill that these events provide in subseasonal to seasonal forecasts (e.g., Tripathi et al. 2015; Butler et al. 2019). In this regard, our findings suggest to look in more detail into lowermost stratospheric dynamics and vortex geometry. New diagnostics based on the position and geometry of the vortex, such as those developed in Lawrence and Manney (2018), have the potential to overcome the difficulty of interpreting latitudinally averaged quantities in largely non-zonal situations such as during stratospheric warmings.

Acknowledgments. This work has been partially funded by the Spanish Ministry of Economy and Innovation grant "PaleoStrat" (CGL2015-69699). AdlC has been supported by the UCM research fellowship *Personal posdoctoral de formación en docencia e investigación en los Departamentos de la UCM*. TB acknowledges support by the U.S. National Science Foundation Climate Dynamics Program (Award 1643167). Data from ERA-20C are available at http://apps.ecmwf.int/datasets/; WACCM output is available at https://www2.acom.ucar.edu/gcm/ccmi-output, and also upon request to the corresponding author.

References

Albers, J. R., and T. Birner, 2014: Vortex Preconditioning due to Planetary and Gravity Waves prior to Sudden Stratospheric Warmings. *J. Atmos. Sci.*, **71 (11)**, 4028–4054, doi:10.1175/JAS-D-14-0026.1.

Andrews, D. G., J. R. Holton, and C. B. Leovy, 1987: *Middle atmosphere dynamics*. Academic Press, San Diego, California, 489 pp.

Attard, H. E., and A. L. Lang, 2019: Troposphere-Stratosphere Coupling Following Tropospheric Blocking and Extratropical Cyclones. *Monthly Weather Review*, doi:10.1175/MWR-D-18-0335.1.

Attard, H. E., R. Rios-Berrios, C. T. Guastini, and A. L. Lang, 2016: Tropospheric and Stratospheric Precursors to the January 2013 Sudden Stratospheric Warming. *Monthly Weather Review*, **144 (4)**, 1321–1339, doi:10.1175/MWR-D-15-0175.1.

Ayarzagüena, B., D. Barriopedro, J. M. GarridoPerez, M. Abalos, A. de la Cámara, R. GarcíaHerrera, N. Calvo, and C. Ordóñez, 2018: Stratospheric Connection to the Abrupt

End of the 2016/2017 Iberian Drought. *Geophysical Research Letters*, **45 (22)**, 12,639–12,646, doi:10.1029/2018GL079802.

Baldwin, M. P., and T. J. Dunkerton, 2001: Stratospheric Harbingers of Anomalous Weather Regimes. *Science*, **294 (5542)**, 581–584, doi:10.1126/science.1063315.

Barriopedro, D., and N. Calvo, 2014: On the Relationship between ENSO, Stratospheric Sudden Warmings, and Blocking. *Journal of Climate*, **27 (12)**, 4704–4720, doi:10.1175/JCLI-D-13-00770.1.

Birner, T., and J. R. Albers, 2017: Sudden Stratospheric Warmings and Anomalous Upward Wave Activity Flux. *SOLA*, **13A (Special_Edition)**, 8–12, doi:10.2151/sola.13A-002.

Butler, A., and Coauthors, 2019: Sub-seasonal Predictability and the Stratosphere. *Sub-Seasonal to Seasonal Prediction*, Elsevier, chap. 11, 223–241, doi:10.1016/B978-0-12-811714-9.00011-5.

Butler, A. H., and L. M. Polvani, 2011: El Niño, La Niña, and stratospheric sudden warmings: A reevaluation in light of the observational record. *Geophysical Research Letters*, **38 (13)**, L13 807, doi:10.1029/2011GL048084.

Butler, A. H., D. J. Seidel, S. C. Hardiman, N. Butchart, T. Birner, and A. Match, 2015: Defining Sudden Stratospheric Warmings. *Bulletin of the American Meteorological Society*, **96 (11)**, 1913–1928, doi:10.1175/BAMS-D-13-00173.1.

Charlton, A. J., and L. M. Polvani, 2007: A New Look at Stratospheric Sudden Warmings. Part I: Climatology and Modeling Benchmarks. *Journal of Climate*, **20 (3)**, 449–469, doi:10.1175/JCLI3996.1.

Charney, J. G., and M. E. Stern, 1962: On the Stability of Internal Baroclinic Jets in a Rotating Atmosphere. *Journal of the Atmospheric Sciences*, **19 (2)**, 159–172, doi:10.1175/1520-0469(1962)019⟨0159:OTSOIB⟩2.0.CO;2.

Chen, M., C. R. Mechoso, and J. D. Farrara, 2001: Interannual variations in the stratospheric circulation with a perfectly steady troposphere. *Journal of Geophysical Research: Atmospheres*, **106 (D6)**, 5161–5172, doi:10.1029/2000JD900624.

Chen, P., and W. A. Robinson, 1992: Propagation of Planetary Waves between the Troposphere and Stratosphere. *Journal of the Atmospheric Sciences*, **49 (24)**, 2533–2545, doi:10.1175/1520-0469(1992)049⟨2533:POPWBT⟩2.0.CO;2.

Christiansen, B., 1999: Stratospheric Vacillations in a General Circulation Model. *Journal of the Atmospheric Sciences*, **56 (12)**, 1858–1872, doi:10.1175/1520-0469(1999)056⟨1858:SVIAGC⟩2.0.CO;2.

Clark, J. H. E., 1974: Atmospheric Response to the Quasi-Resonant of Forced Planetary Waves. *Journal of the Meteorological Society of Japan*, **52 (2)**, 143–162.

Colucci, S. J., and M. E. Kelleher, 2015: Diagnostic Comparison of Tropospheric Blocking Events with and without Sudden Stratospheric Warming. *Journal of the Atmospheric Sciences*, **72 (6)**, 2227–2240, doi:10.1175/JAS-D-14-0160.1.

Compo, G. P., J. S. Whitaker, and P. D. Sardeshmukh, 2006: Feasibility of a 100-Year Reanalysis Using Only Surface Pressure Data. *Bulletin of the American Meteorological Society*, **87 (2)**, 175–190, doi:10.1175/BAMS-87-2-175.

de la Cámara, A., M. Abalos, and P. Hitchcock, 2018a: Changes in Stratospheric Transport and Mixing During Sudden Stratospheric Warmings. *Journal of Geophysical Research: Atmospheres*, **123 (7)**, 3356–3373, doi:10.1002/2017JD028007.

de la Cámara, A., M. Abalos, P. Hitchcock, N. Calvo, and R. R. Garcia, 2018b: Response of Arctic ozone to sudden stratospheric warmings. *Atmospheric Chemistry and Physics*, **18 (22)**, 16 499–16 513, doi:10.5194/acp-18-16499-2018.

de la Cámara, A., J. R. Albers, T. Birner, R. R. Garcia, P. Hitchcock, D. E. Kinnison, and A. K. Smith, 2017: Sensitivity of Sudden Stratospheric Warmings to Previous Stratospheric Conditions. *Journal of the Atmospheric Sciences*, **74 (9)**, 2857–2877, doi:10.1175/JAS-D-17-0136.1.

Domeisen, D. I. V., C. I. Garfinkel, and A. H. Butler, 2018a: The Teleconnection of El Niño Southern Oscillation to the Stratosphere. *Reviews of Geophysics*, doi:10.1029/2018RG000596.

Domeisen, D. I. V., O. Martius, and B. Jiménez-Esteve, 2018b: Rossby Wave Propagation into the Northern Hemisphere Stratosphere: The Role of Zonal Phase Speed. *Geophysical Research Letters*, **45 (4)**, 2064–2071, doi:10.1002/2017GL076886.

Esler, J. G., and N. J. Matthewman, 2011: Stratospheric Sudden Warmings as Self-Tuning Resonances. Part II: Vortex Displacement Events. *Journal of the Atmospheric Sciences*, **68 (11)**, 2505–2523, doi:10.1175/JAS-D-11-08.1.

Garcia, R. R., A. K. Smith, D. E. Kinnison, A. de la Cámara, and D. J. Murphy, 2017: Modification of the Gravity Wave Parameterization in the Whole Atmosphere Community Climate Model: Motivation and Results. *Journal of the Atmospheric Sciences*, **74 (1)**, 275–291, doi:10.1175/JAS-D-16-0104.1.

Garfinkel, C. I., A. H. Butler, D. W. Waugh, M. M. Hurwitz, and L. M. Polvani, 2012: Why might stratospheric sudden warmings occur with similar frequency in El Niño and La Niña winters? *Journal of Geophysical Research: Atmospheres*, **117 (D19)**, n/a–n/a, doi:10.1029/2012JD017777.

Garfinkel, C. I., C. Schwartz, D. I. V. Domeisen, S.-W. Son, A. H. Butler, and I. P. White, 2018: Extratropical Atmospheric Predictability From the Quasi-Biennial Oscillation in Subseasonal Forecast Models. *Journal of Geophysical Research: Atmospheres*, **123 (15)**, 7855–7866, doi:10.1029/2018JD028724.

Hitchcock, P., and P. H. Haynes, 2016: Stratospheric control of planetary waves. *Geophysical Research Letters*, **43 (22)**, 11,884–11,892, doi:10.1002/2016GL071372.

Holton, J. R., and C. Mass, 1976: Stratospheric vacillation cycles. *Journal of the Atmospheric Sciences*, **33**, 2218–2225.

Jucker, M., 2016: Are Sudden Stratospheric Warmings Generic? Insights from an Idealized GCM. *Journal of the Atmospheric Sciences*, **73 (12)**, 5061–5080, doi:10.1175/JAS-D-15-0353.1.

Kidston, J., A. a. Scaife, S. C. Hardiman, D. M. Mitchell, N. Butchart, M. P. Baldwin, and L. J. Gray, 2015: Stratospheric influence on tropospheric jet streams, storm tracks and surface weather. *Nature Geoscience*, **8 (6)**, 433–440, doi:10.1038/ngeo2424.

Labitzke, K., 1977: Interannual Variability of the Winter Stratosphere in the Northern Hemisphere. *Monthly Weather Review*, **105 (6)**, 762–770, doi:10.1175/1520-0493(1977)105⟨0762:IVOTWS⟩2.0.CO;2.

Labitzke, K., 1978: On the Different Behavior of the Zonal Harmonic Height Waves 1 and 2 During the Winters 1970/71 and 1971/72. *Monthly Weather Review*, **106 (12)**, 1704–1713, doi:10.1175/1520-0493(1978)106⟨1704:OTDBOT⟩2.0.CO;2.

Labitzke, K., 1981: Stratospheric-mesospheric midwinter disturbances: A summary of observed characteristics. *Journal of Geophysical Research*, **86 (C10)**, 9665, doi:10.1029/JC086iC10p09665.

Lawrence, Z. D., and G. L. Manney, 2018: Characterizing Stratospheric Polar Vortex Variability With Computer Vision Techniques. *Journal of Geophysical Research: Atmospheres*, **123 (3)**, 1510–1535, doi:10.1002/2017JD027556.

Lindgren, E. A., A. Sheshadri, and R. A. Plumb, 2018: Sudden Stratospheric Warming Formation in an Idealized General Circulation Model Using Three Types of Tropospheric Forcing. *Journal of Geophysical Research: Atmospheres*, **123 (18)**, 10,125–10,139, doi:10.1029/2018JD028537.

Marsh, D. R., M. J. Mills, D. E. Kinnison, J.-F. Lamarque, N. Calvo, and L. M. Polvani, 2013: Climate Change from 1850 to 2005 Simulated in CESM1(WACCM). *Journal of Climate*, **26 (19)**, 7372–7391, doi:10.1175/JCLI-D-12-00558.1.

Marshall, A. G., and A. A. Scaife, 2010: Improved predictability of stratospheric sudden warming events in an atmospheric general circulation model with enhanced stratospheric resolution. *Journal of Geophysical Research*, **115**, D16 114, doi:10.1029/2009JD012643.

Martineau, P., G. Chen, S.-W. Son, and J. Kim, 2018a: Lower-Stratospheric Control of the Frequency of Sudden Stratospheric Warming Events. *Journal of Geophysical Research: Atmospheres*, **123 (6)**, 3051–3070, doi:10.1002/2017JD027648.

516 Martineau, P., and S.-W. Son, 2015: Onset of Circulation Anomalies during Stratospheric Vortex
517 Weakening Events: The Role of Planetary-Scale Waves. *Journal of Climate*, **28 (18)**, 7347–
518 7370, doi:10.1175/JCLI-D-14-00478.1.

519 Martineau, P., J. S. Wright, N. Zhu, and M. Fujiwara, 2018b: Zonal-mean data set of global
520 atmospheric reanalyses on pressure levels. *Earth System Science Data*, **10 (4)**, 1925–1941, doi:
521 10.5194/essd-10-1925-2018.

522 Martius, O., L. M. Polvani, and H. C. Davies, 2009: Blocking precursors to stratospheric sudden
523 warming events. *Geophysical Research Letters*, **36 (14)**, L14 806, doi:10.1029/2009GL038776.

524 Matsuno, T., 1971: A Dynamical Model of the Stratospheric Sudden Warming. *Journal of the*
525 *Atmospheric Sciences*, **28 (8)**, 1479–1494, doi:10.1175/1520-0469(1971)028⟨1479:ADMOTS⟩
526 2.0.CO;2.

527 Matthewman, N. J., and J. G. Esler, 2011: Stratospheric Sudden Warmings as Self-Tuning Res-
528 onances. Part I: Vortex Splitting Events. *Journal of the Atmospheric Sciences*, **68 (11)**, 2481–
529 2504, doi:10.1175/JAS-D-11-07.1.

530 Matthewman, N. J., J. G. Esler, A. J. Charlton-Perez, and L. M. Polvani, 2009: A New Look at
531 Stratospheric Sudden Warmings. Part III: Polar Vortex Evolution and Vertical Structure. *Journal*
532 *of Climate*, **22 (6)**, 1566–1585, doi:10.1175/2008JCLI2365.1.

533 McIntyre, M. E., 1982: How Well do we Understand the Dynamics of Stratospheric Warmings?
534 *Journal of the Meteorological Society of Japan. Ser. II*, **60 (1)**, 37–65, doi:10.2151/jmsj1965.
535 60.1_37.

536 Melander, M. V., N. J. Zabusky, and A. S. Styczek, 1986: A moment model for vortex in-
537 teractions of the two-dimensional Euler equations. Part 1. Computational validation of a

Hamiltonian elliptical representation. *Journal of Fluid Mechanics*, **167**, 95–115, doi:10.1017/S0022112086002744.

Newman, P. A., and J. E. Rosenfield, 1997: Stratospheric thermal damping times. *Geophysical Research Letters*, **24 (4)**, 433–436, doi:10.1029/96GL03720.

Plumb, R. A., 1981: Instability of the Distorted Polar Night Vortex: A Theory of Stratospheric Warmings. *Journal of the Atmospheric Sciences*, **38 (11)**, 2514–2531, doi:10.1175/1520-0469(1981)038⟨2514:IOTDPN⟩2.0.CO;2.

Poli, P., and Coauthors, 2016: ERA-20C: An Atmospheric Reanalysis of the Twentieth Century. *Journal of Climate*, **29 (11)**, 4083–4097, doi:10.1175/JCLI-D-15-0556.1.

Polvani, L. M., and D. W. Waugh, 2004: Upward Wave Activity Flux as a Precursor to Extreme Stratospheric Events and Subsequent Anomalous Surface Weather Regimes. *Journal of Climate*, **17 (18)**, 3548–3554, doi:10.1175/1520-0442(2004)017⟨3548:UWAFAA⟩2.0.CO;2.

Scaife, a. a., and Coauthors, 2014: Skillful long range prediction of European and North American winters. *Geophysical Research Letters*, **5**, 2514–2519, doi:10.1002/2014GL059637.Received.

Scaife, A. A., and Coauthors, 2016: Seasonal winter forecasts and the stratosphere. *Atmospheric Science Letters*, **17 (1)**, 51–56, doi:10.1002/asl.598.

Scott, R. K., and P. H. Haynes, 2000: Internal Vacillations in Stratosphere-Only Models. *Journal of the Atmospheric Sciences*, **57 (19)**, 3233–3250, doi:10.1175/1520-0469(2000)057⟨3233:IVISOM⟩2.0.CO;2.

Scott, R. K., and L. M. Polvani, 2004: Stratospheric control of upward wave flux near the tropopause. *Geophysical Research Letters*, **31 (2)**, L02 115, doi:10.1029/2003GL017965.

559 Scott, R. K., and L. M. Polvani, 2006: Internal Variability of the Winter Stratosphere. Part I: Time-
560 Independent Forcing. *Journal of the Atmospheric Sciences*, **63 (11)**, 2758–2776, doi:10.1175/
561 JAS3797.1.

562 Sjoberg, J. P., and T. Birner, 2012: Transient tropospheric forcing of sudden stratospheric warm-
563 ings. *Journal of the Atmospheric Sciences*, **69 (1976)**, 3420–3432, doi:10.1175/JAS-D-11-0195.
564 1.

565 Sjoberg, J. P., and T. Birner, 2014: Stratospheric Wave-Mean Flow Feedbacks and Sudden Strato-
566 spheric Warmings in a Simple Model Forced by Upward Wave Activity Flux. *Journal of the*
567 *Atmospheric Sciences*, **71 (11)**, 4055–4071, doi:10.1175/JAS-D-14-0113.1.

568 Smith, A. K., 1983: Observation of Wave-Wave Interactions in the Stratosphere. *Journal of the At-*
569 *mospheric Sciences*, **40 (10)**, 2484–2496, doi:10.1175/1520-0469(1983)040⟨2484:OOWWII⟩2.
570 0.CO;2.

571 Smith, A. K., 1989: An Investigation of Resonant Waves in a Numerical Model of an Observed
572 Sudden Stratospheric Warming. *Journal of the Atmospheric Sciences*, **46 (19)**, 3038–3054, doi:
573 10.1175/1520-0469(1989)046⟨3038:AIORWI⟩2.0.CO;2.

574 Smith, A. K., 1992: Precoditioning for stratospheric sudden warmings: Sensitivity studies with a
575 numerical model. *Journal of the Atmospheric Sciences*, **49 (12)**, 1003–1019.

576 Smith, A. K., J. C. Gille, and L. V. Lyjak, 1984: WaveWave Interactions in the Stratosphere:
577 Observations during Quiet and Active Wintertime Periods. *Journal of the Atmospheric Sciences*,
578 **41 (3)**, 363–373, doi:10.1175/1520-0469(1984)041⟨0363:WIITSO⟩2.0.CO;2.

Smith, K. L., and P. J. Kushner, 2012: Linear interference and the initiation of extratropical stratosphere-troposphere interactions. *Journal of Geophysical Research Atmospheres*, **117 (13)**, 1–16, doi:10.1029/2012JD017587,2012.

Thompson, D. W. J., M. P. Baldwin, and J. M. Wallace, 2002: Stratospheric Connection to Northern Hemisphere Wintertime Weather: Implications for Prediction. *Journal of Climate*, **15 (12)**, 1421–1428, doi:10.1175/1520-0442(2002)015⟨1421:SCTNHW⟩2.0.CO;2.

Tripathi, O. P., and Coauthors, 2015: The predictability of the extratropical stratosphere on monthly time-scales and its impact on the skill of tropospheric forecasts. *Quarterly Journal of the Royal Meteorological Society*, **141 (689)**, 987–1003, doi:10.1002/qj.2432.

Tung, K. K., and R. S. Lindzen, 1979: A Theory of Stationary Long Waves. Part II: Resonant Rossby Waves in the Presence of Realistic Vertical Shears. *Monthly Weather Review*, **107 (6)**, 735–750, doi:10.1175/1520-0493(1979)107⟨0735:ATOSLW⟩2.0.CO;2.

Waugh, D. N. W., 1997: Elliptical diagnostics of stratospheric polar vortices. *Quarterly Journal of the Royal Meteorological Society*, **123 (542)**, 1725–1748, doi:10.1002/qj.49712354213.

White, I., C. I. Garfinkel, E. P. Gerber, M. Jucker, V. Aquila, and L. D. Oman, 2019: The Downward Influence of Sudden Stratospheric Warmings: Association with Tropospheric Precursors. *Journal of Climate*, **32 (1)**, 85–108, doi:10.1175/JCLI-D-18-0053.1.

Yoden, S., 1987: Dynamical Aspects of Stratospheric Vacillations in a Highly Truncated Model. *Journal of the Atmospheric Sciences*, **44 (24)**, 3683–3695, doi:10.1175/1520-0469(1987)044⟨3683:DAOSVI⟩2.0.CO;2.

LIST OF TABLES

		LTWE1	LTWE2	All LTWE
WACCM	Followed by SSD	50 (26%)	22 (12%)	72 (19%)
	Not followed by SSD	144 (74%)	157 (88%)	301 (81%)
	Total	194	179	373
ERA-20C	Followed by SSD	21 (30%)	7 (8%)	28 (17%)
	Not followed by SSD	50 (70%)	84 (92%)	134 (83%)
	Total	71	91	162

603 TABLE 1. Number of lower tropospheric wave events (LTWEs) followed and not followed by sudden strato-
604 spheric deceleration (SSD) events.

		SSD1	SSD2	SSD1&2	SSDww	All SSD
WACCM	Preceded by LTWE1	39 (38%)	2 (6%)	0 (-)	13 (21%)	54 (27%)
	Preceded by LTWE2	6 (6%)	9 (28%)	0 (-)	5 (8%)	20 (10%)
	Not preceded by LTWE	61 (58%)	27 (66%)	0 (-)	44 (71%)	126 (63%)
	Total	106	32	0	62	200
ERA-20C	Preceded by LTWE1	18 (40%)	1 (6%)	0 (0%)	4 (13%)	23 (24%)
	Preceded by LTWE2	1 (2%)	5 (29%)	1 (33%)	1 (3%)	8 (8%)
	Not preceded by LTWE	26 (58%)	11 (65%)	2 (67%)	25 (83%)	64 (67%)
	Total	45	17	3	30	95

TABLE 2. Number of SSDs preceded and not preceded by LTWEs.

LIST OF FIGURES

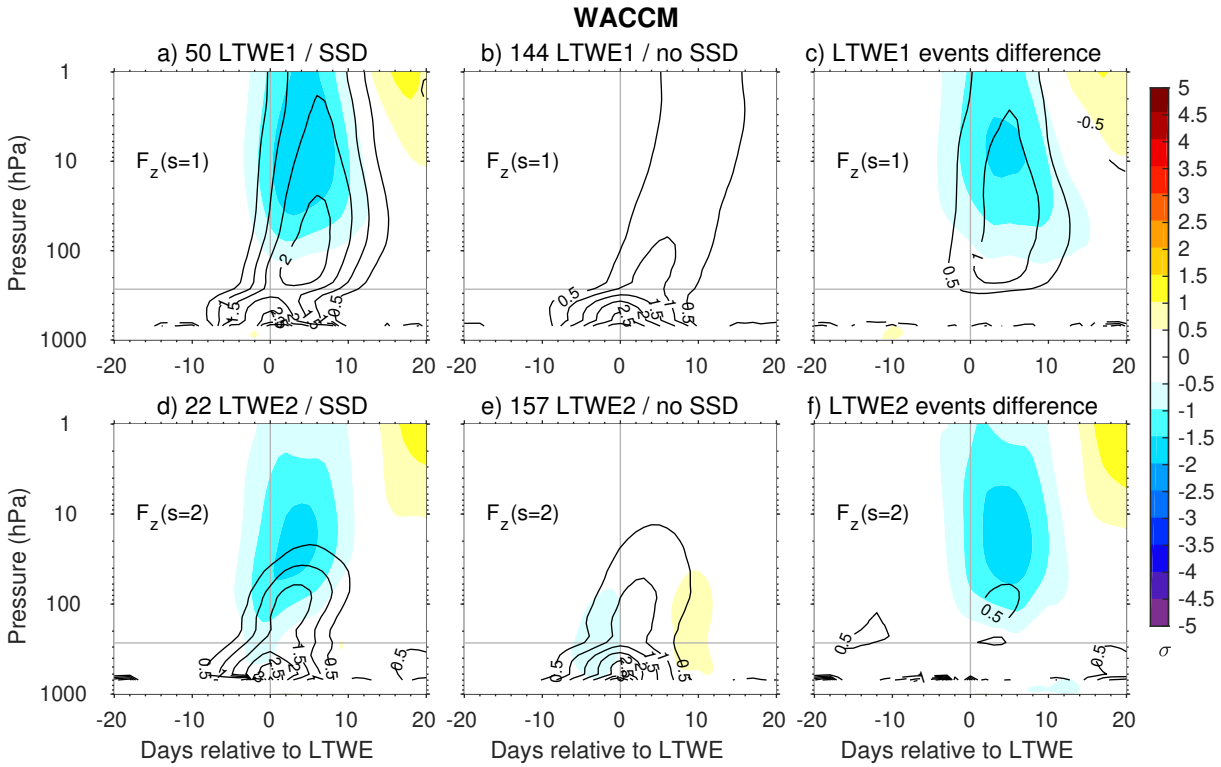

FIG. 1. Composite evolution, as a function of lag and pressure level, for extreme upward wave activity events (LTWEs) near 600 hPa in WACCM. The upward EP flux anomaly is shown in black contours (quantized in individual zonal wavenumbers, as indicated), with the 10-day integrated wind tendency in colors. (Left; a, d) Subset of those LTWEs associated with an SSW. (Middle; b, e) Subset of those LTWEs not associated with SSWs. (Right; c, f) Difference between (left) and (middle). Top row (a-c) shows LTWE1, bottom row (d-f) shows LTWE2. All anomalies are standardized, i.e. high values indicate high statistical significance. Horizontal gray line marks approximate tropopause level (∼270 hPa).

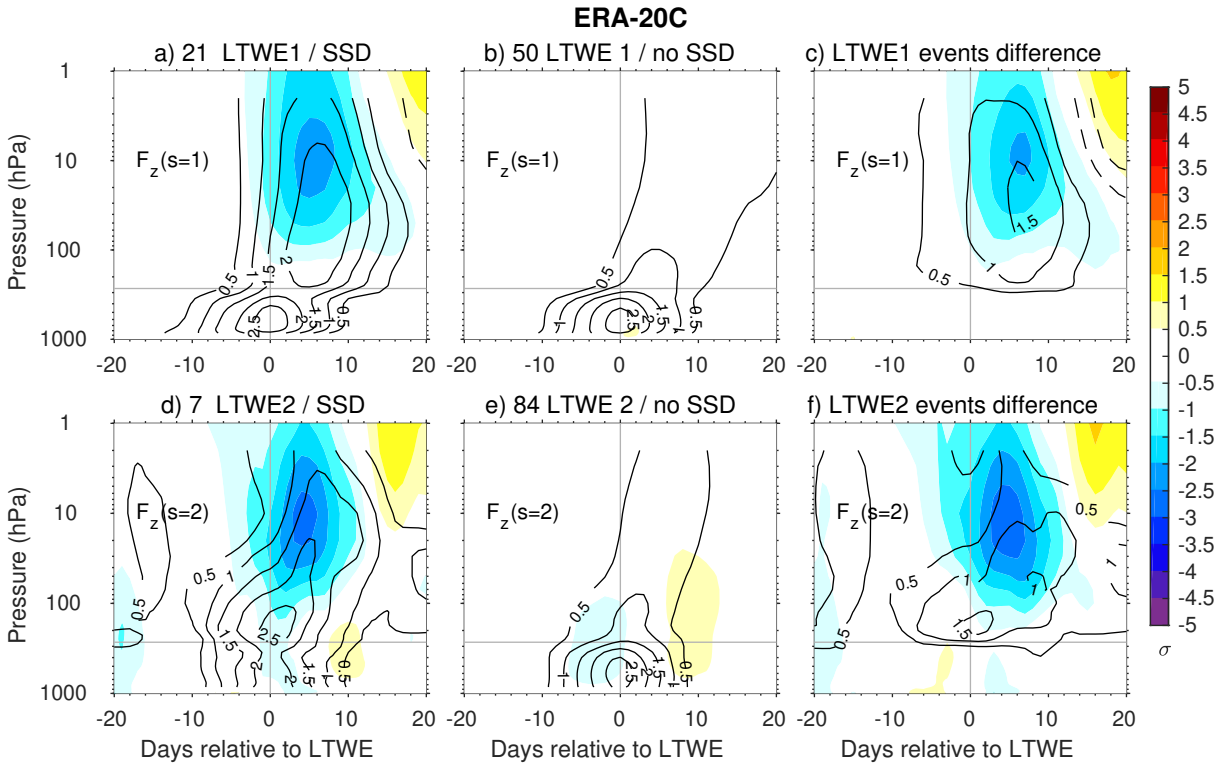

FIG. 2. As in Fig. 1, but for ERA-20C.

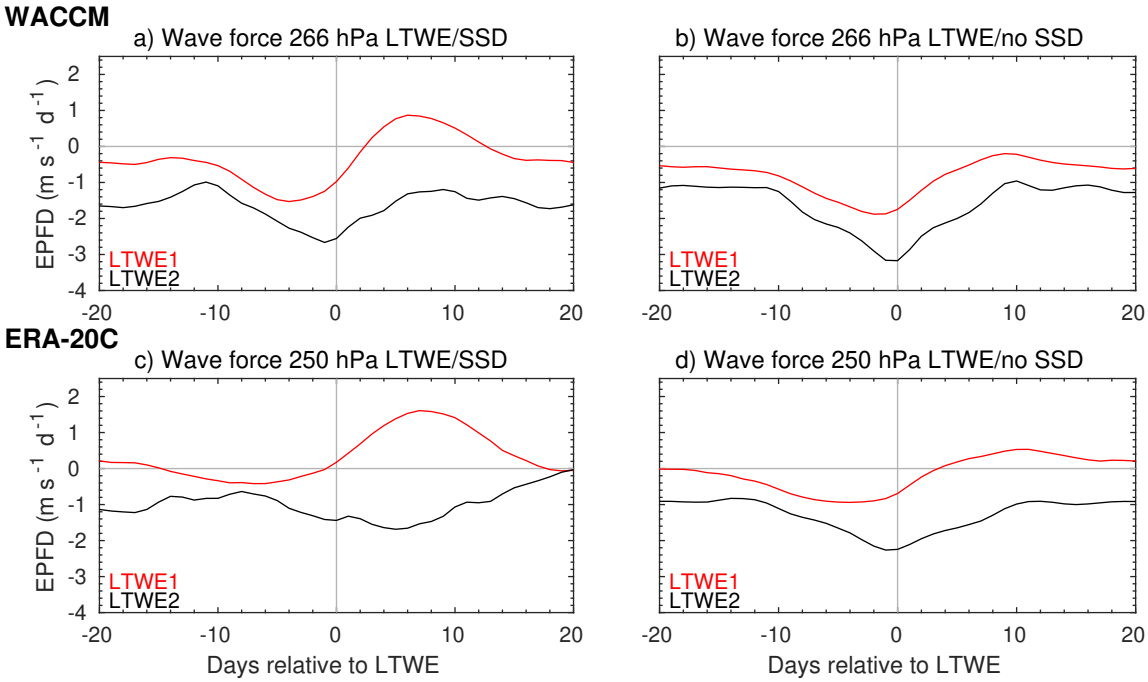

654 FIG. 3. Time evolution of the EP flux divergence (EPFD) (net values, no anomalies) at ∼266 hPa around the
655 LTWE central date. EPFD of the zonal harmonic s=1 is displayed for LTWE1 (red line), and zonal harmonic
656 s=2 for LTWE2 (black lines). Composite evolution for LTWEs followed and not followed by SSDs is shown in
657 the left and right panels, respectively.

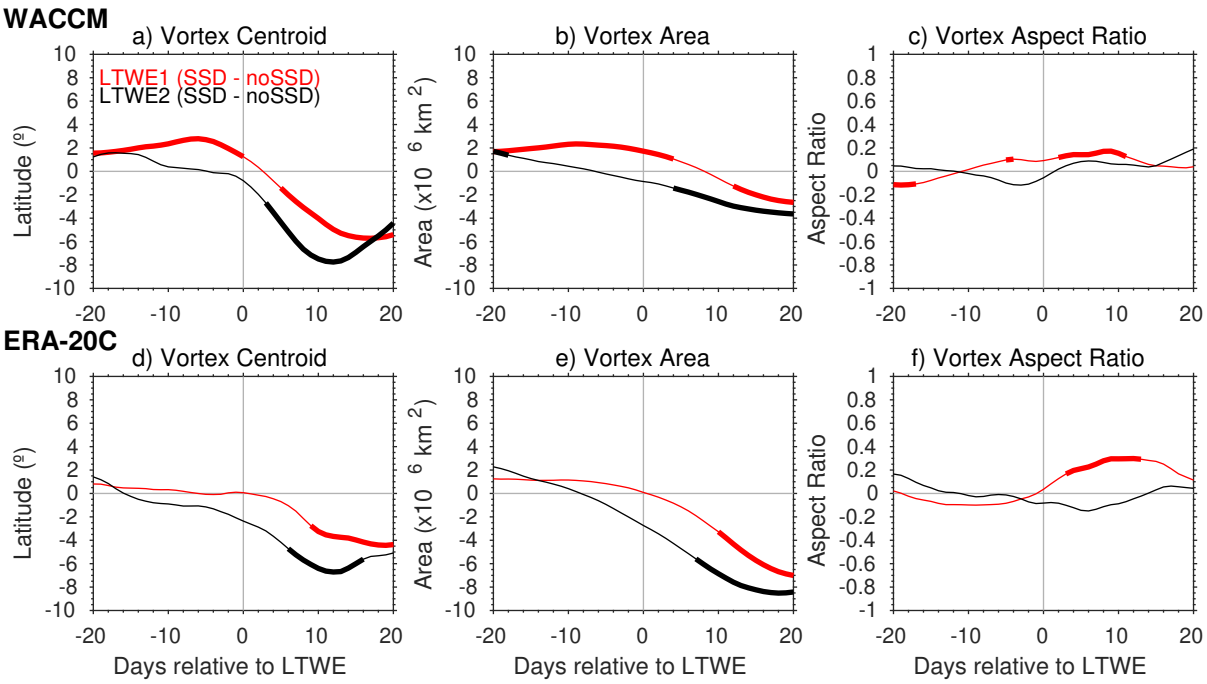

658 FIG. 4. Composite evolution around LTWE central dates of anomalies of elliptical diagnostics at 850 K: (Left;
659 a, d) latitude of the vortex centroid, (middle; b, e) vortex area, and (right; c, f) vortex aspect ratio. Red (black)
660 lines indicate the composite difference between LTWE1 (LTWE2) followed and not followed by SSWs, with
661 thick lines highlighting the statistically significant values (Student t-test for the difference of means, $\alpha = 0.05$).
662 Results for WACCM and ERA-20C are shown in the top and bottom panels, respectively.

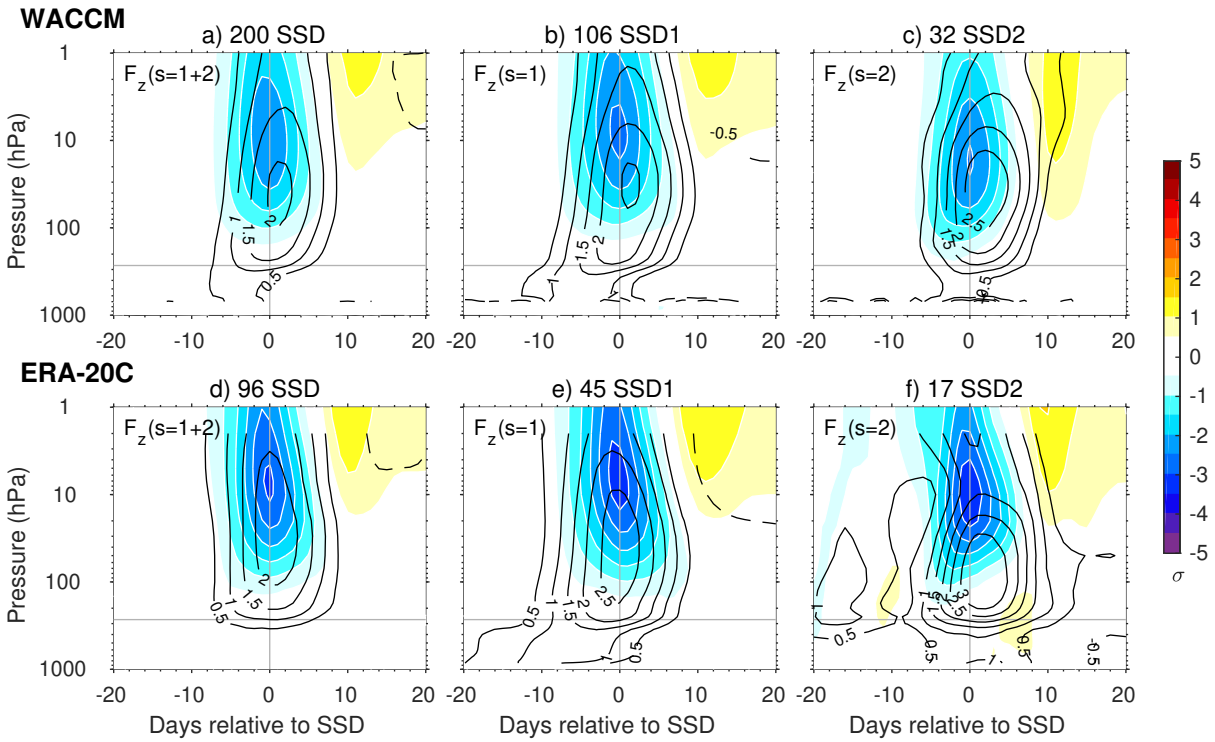

663 FIG. 5. Composite evolution, as a function of lag and pressure level, for (left; a, d) all SSW events, (middle;
664 b, e) SSW1 events, and (right; c, f) SSW2 events in (top) WACCM and (bottom) ERA-20C. The upward EP flux
665 anomaly is shown in black contours, and the anomalies of the 10-day integrated wind tendency in colors. All
666 anomalies are standardized, i.e. high values indicate high statistical significance. Horizontal gray lines mark the
667 approximate tropopause level (∼270 hPa).

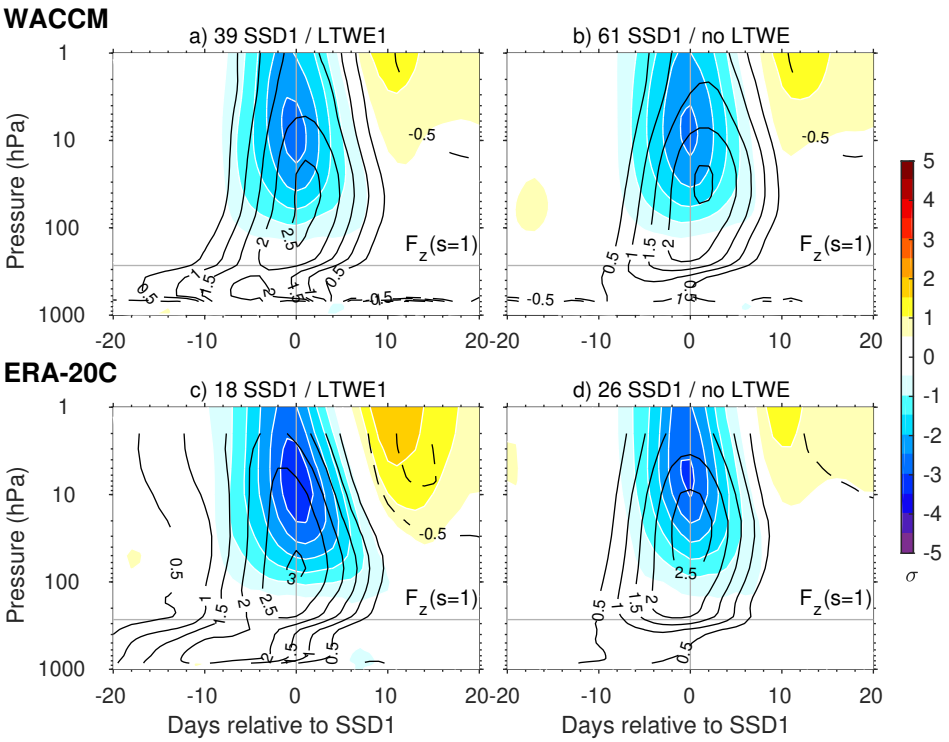

668 FIG. 6. Composite evolution, as a function of lag and pressure level, for (left; a, c) SSW1 preceded by LTWE1,
669 and (right; b, d) SSW1 not preceded by LTWEs, in (top) WACCM and (bottom) ERA-20C. The upward EP flux
670 anomaly (for zonal wavenumber 1 $F_z(s=1)$) is shown in black contours, and the anomalies of the 10-day
671 integrated wind tendency in colors. All anomalies are standardized, i.e. high values indicate high statistical
672 significance. Horizontal gray lines mark the approximate tropopause level (∼270 hPa).

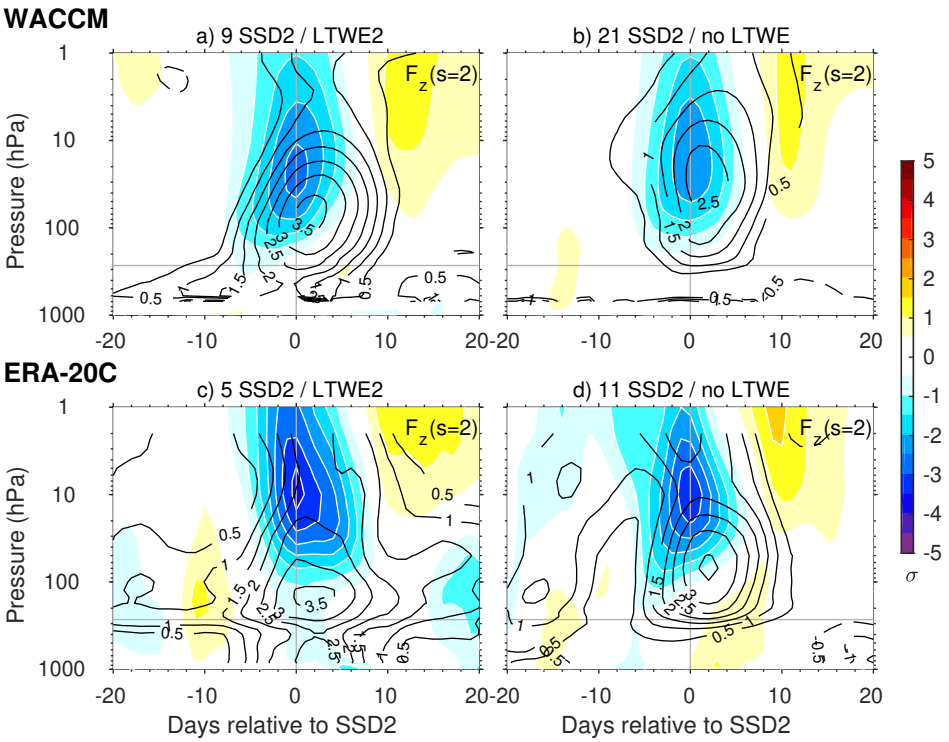

673 FIG. 7. As in Fig. 6 but for SSW2 events, and black contours showing anomalies of upward wave activity for
674 zonal wavenumber 2 ($F_z(s=2)$).

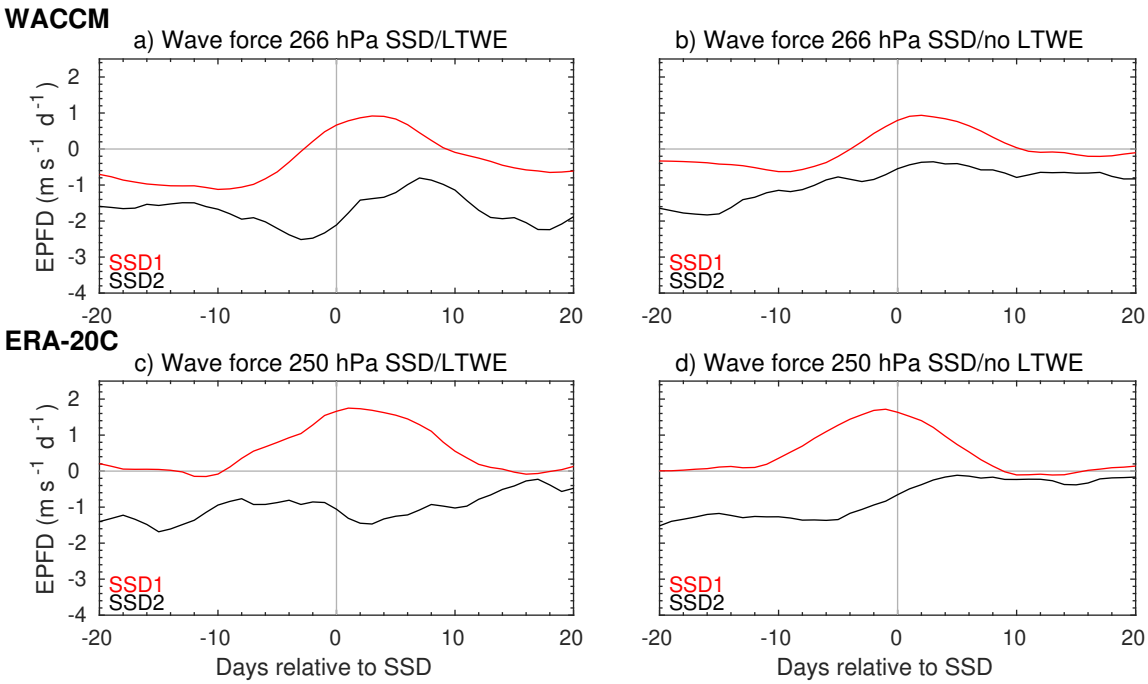

FIG. 8. As in Fig. 3, but for SSD events preceded and not by LTWEs.

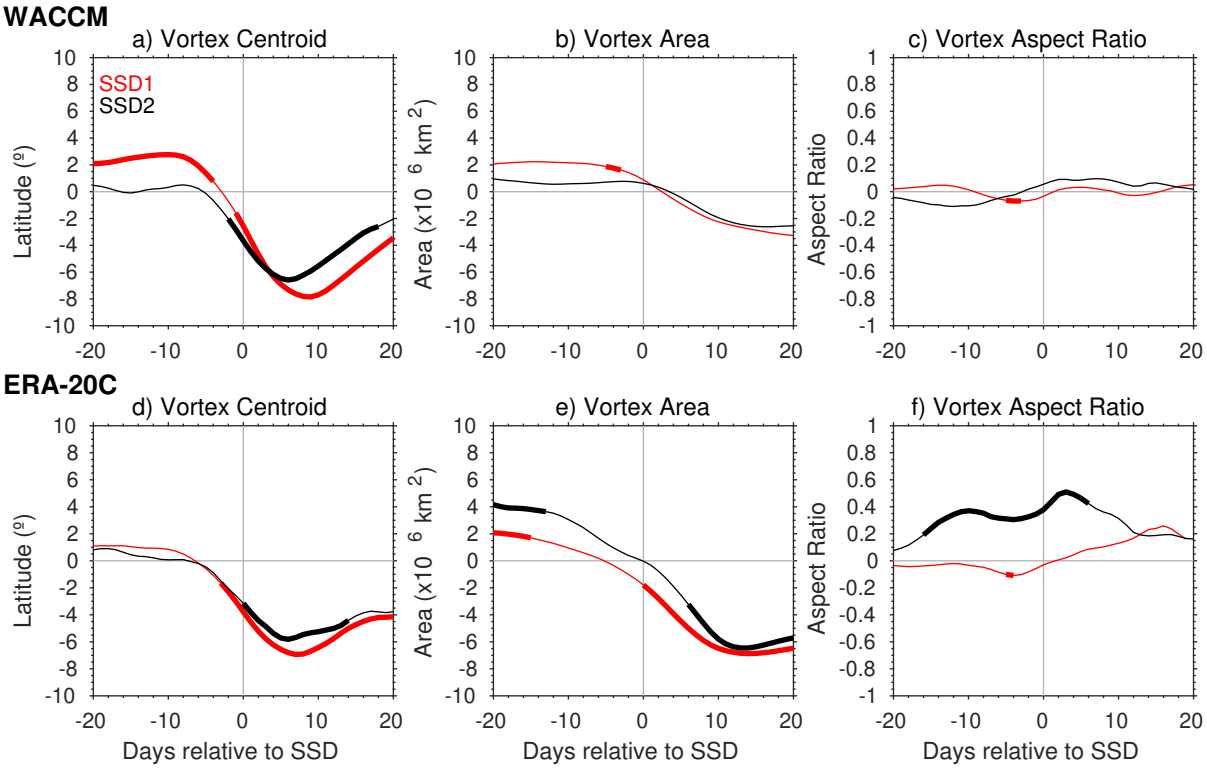

675 FIG. 9. Composite evolution around SSD central dates of anomalies of elliptical diagnostics at 850 K: (Left;
676 a, d) latitude of the vortex centroid, (middle; b, e) vortex area, and (right; c, f) vortex aspect ratio. Red and black
677 lines indicate the composite anomalies for all SSD1 and SSD2, respectively, with thick lines highlighting the
678 statistically significant values (Student t-test, $\alpha = 0.05$). Results for WACCM and ERA-20C are shown in the
679 top and bottom panels, respectively.